Journal of the American Heart Association

ORIGINAL RESEARCH

Localized Antileptin Therapy Prevents Aortic Root Dilatation and Preserves Left Ventricular Systolic Function in a Murine Model of Marfan Syndrome

Sudeshna Fisch, PhD; Noa Bachner-Hinenzon, PhD; Offir Ertracht, PhD; Liang Guo, MD; Yhara Arad, MSc; Danny Ben-Zvi, PhD; Ronglih Liao, PhD; Jacob Schneiderman, MD

BACKGROUND: Marfan syndrome (MFS) is a genetically transmitted connective tissue disorder characterized by aortic root dilatation, dissection, and rupture. Molecularly, MFS pathological features have been shown to be driven by increased angiotensin II in the aortic wall. Using an angiotensin II–driven aneurysm mouse model, we have recently demonstrated that local inhibition of leptin activity restricts aneurysm formation in the ascending and abdominal aorta. As we observed de novo leptin synthesis in the ascending aortic aneurysm wall of patients with MFS, we hypothesized that local counteracting of leptin activity in MFS may also prevent aortic cardiovascular complications in this context.

METHODS AND RESULTS: *Fbn1*$^{C1039G/+}$ mice underwent periaortic application of low-dose leptin antagonist at the aortic root. Treatment abolished medial degeneration and prevented increase in aortic root diameter (P<0.001). High levels of leptin, transforming growth factor β1, Phosphorylated Small mothers against decapentaplegic 2, and angiotensin-converting enzyme 1 observed in saline-treated MFS mice were downregulated in leptin antagonist–treated animals (P<0.01, P<0.05, P<0.001, and P<0.001, respectively). Leptin and angiotensin-converting enzyme 1 expression levels in left ventricular cardiomyocytes were also decreased (P<0.001) and coincided with prevention of left ventricular hypertrophy and aortic and mitral valve leaflet thickening (P<0.01 and P<0.05, respectively) and systolic function preservation.

CONCLUSIONS: Local, periaortic application of leptin antagonist prevented aortic root dilatation and left ventricular valve remodeling, preserving left ventricular systolic function in an MFS mouse model. Our results suggest that local inhibition of leptin may constitute a novel, stand-alone approach to prevent MFS aortic root aneurysms and potentially other similar angiotensin II–driven aortic pathological features.

Key Words: aortic aneurysm ■ leptin antagonist ■ local therapy ■ Marfan syndrome ■ systolic dysfunction

Marfan syndrome (MFS) is an autosomal dominant disease of connective tissue found in 1:5000 individuals, presenting clinically with musculoskeletal, ocular, and cardiovascular manifestations. Progressive dilatation of the aortic root in patients with MFS results in aneurysm formation, which is susceptible to dissection and subsequent fatal rupture. MFS-related cardiovascular manifestations often include cardiac dysfunction, myxomatous degeneration of the mitral and aortic valve leaflets, and main pulmonary artery (MPA) dilatation.[1]

MFS is associated with mutations in the *FBN1* gene, which encodes fibrillin-1 microfibrils, a major component of the extracellular matrix (ECM). For the past decade, this syndrome has been attributed to excessive transforming growth factor β (TGFβ) signaling in the

Correspondence to: Jacob Schneiderman, MD, Department of Vascular Surgery, Sheba Medical Center, Tel Hashomer 52621, Israel. E-mail: jschneid@post.tau.ac.il

Supplementary Materials for this article are available at https://www.ahajournals.org/doi/suppl/10.1161/JAHA.119.014761

For Sources of Funding and Disclosures, see page 17.

JAHA is available at: www.ahajournals.org/journal/jaha

CLINICAL PERSPECTIVE

What Is New?

- Periarterial application of a leptin antagonist at the aortic root prevents local medial degeneration and aneurysm formation in Marfan syndrome mice. Inhibition of leptin activity in the aortic root likely downregulated local angiotensin II signaling via reduction of leptin, angiotensin-converting enzyme 1, and transforming growth factor β expression in the vessel wall.
- Preservation of aortic root integrity in Marfan syndrome mice prevented left ventricular hypertrophy and remodeling of left ventricular valve leaflets, contributing to rescue left ventricular systolic function by reducing angiotensin-converting enzyme 1 and leptin expression in left ventricular cardiomyocytes.

What Are the Clinical Implications?

- Local inhibition of leptin activity in the vessel wall may constitute an effective stand-alone therapeutic strategy to attenuate the formation of angiotensin II/transforming growth factor β–driven aortic or peripheral aneurysms.

Nonstandard Abbreviations and Acronyms

AAA	abdominal aortic aneurysm
ACE-1	angiotensin-converting enzyme 1
ACE-2	angiotensin-converting enzyme 2
AngII	angiotensin II
AR	aortic regurgitation
AT1R	angiotensin type 1 receptor
ECM	extracellular matrix
EDD	end diastolic diameter
EF	ejection fraction
ESD	end systolic diameter
FAC	fractional area change
Fbn1	fibrillin 1
FS	fractional shortening
LepA	leptin antagonist
LV	left ventricular
MFS	Marfan syndrome
MMP	matrix metalloproteinase
MPA	main pulmonary artery
PLGA	poly lactic-co-glycolic acid
pSmad2	small mothers against decapentaplegic 2
SBP	systolic blood pressure
SMC	smooth muscle cell
TGFβ	transforming growth factor β
WT	wild type

vessel wall.[2,3] TGFβ family cytokines are secreted as large, latent complexes, which are bound to the ECM by fibrillin-1 microfibrils. In response to inflammatory proteolysis, fibrillin-1 microfibrils are degraded, which releases latent TGFβ from the ECM and increases its bioavailability. In MFS, reduced or abnormal fibrillin-1 leads to a failure in TGFβ sequestration and overactive signaling. These events are associated with modulation of the vascular smooth muscle cell (SMC) phenotype, dysregulation of ECM synthesis, and degenerative changes in the vessel wall.[4]

It remains unclear whether TGFβ drives MFS aortic root aneurysm pathological features. In a seminal study, inhibition of TGFβ with neutralizing antibodies prevented aortic root dilatation in adult MFS mice (*Fbn1*$^{C1039G/+}$), suggesting that it has a causal role in the process.[5] Additional experiments using these mice revealed the involvement of a noncanonical, Small mothers against decapentaplegic (Smad) 2-independent TGFβ signaling pathway in nonmyocyte heart cells[6] and SMC. TGFβ has also been implicated in the early stages of aortic aneurysm development.[7] However, an experiment in young MFS mice found no elevated TGFβ signaling in aortic SMCs.[8] Moreover, a study of patients with MFS showed a reverse correlation between plasma TGFβ levels and increased aortic dilatation.[9] Wider analysis of aneurysm samples from syndromic (such as MFS) and nonsyndromic diseases found that both exhibit increased levels of TGFβ and phosphorylated Smad2.[10] These later findings suggest that overactive TGFβ signaling may merely reflect degenerative processes in the vessel wall, which are unrelated to mutation of *FBN1*.

As opposed to the controversial role of TGFβ in aortic aneurysm formation, it is clear that MFS-induced pathological cardiovascular manifestations are driven by activated angiotensin II (AngII) signaling pathway in aortic SMCs and cardiomyocytes. AngII signaling occurs mostly through binding to the AngII type 1 receptor (AT1R) and drives aortic and cardiac remodeling.[11] AngII is known to induce TGFβ and TGFβ receptor expression in a variety of tissues, including the aorta,[12] thereby contributing to degenerative changes in the vessel wall and increasing systemic levels of TGFβ.[13]

We have previously shown that remodeling in human cardiovascular organs, like rupture-prone atherosclerotic plaques in carotid arteries, is associated with local induction of leptin.[14] We have also demonstrated that leptin drives the formation of abdominal and ascending aortic aneurysms in apolipoprotein E–deficient mice.[15,16] As a local mediator of AngII-induced cardiovascular remodeling, leptin promotes TGFβ induction,[17] generates reactive oxygen species,[18] and elicits recruitment of inflammatory cells, which produce and activate matrix metalloproteinases (MMPs).[19,20]

Collectively, these factors promote medial degeneration, aneurysm formation, and aortic dissection.[21]

We have previously demonstrated that local inhibition of leptin activity prevents ascending aortic aneurysm in apolipoprotein E–deficient mice, and that human MFS aortic aneurysm samples have increased local leptin gene expression.[16] Therefore, we hypothesized that MFS-associated aortic aneurysms may be prevented by local inhibition of leptin activity. The current study evaluates local periaortic antileptin therapy as a novel approach to preventing the development of aortic root aneurysm in MFS mice.

METHODS

Data are available on request from the corresponding author.

The Mouse Model

Fbn1$^{C1093G/+}$ heterozygous Marfan mice (MFS mice) (stock No. 012885) were generated at Jackson Labs (Bar Harbor, MN) by in vitro fertilization. Six-week-old male Marfan heterozygous (n=23), and wild-type (WT) littermates (n=4) were shipped to the Brigham and Women's Hospital Non-Barrier Housing facility in Boston, MA. The experiment was performed in accordance with the guidelines of Brigham and Women's Hospital Institutional Animal Care and Use Committee and under Brigham and Women's Hospital protocol 2016N2000266.

After 7 days of acclimatization, all 7-week old mice underwent a baseline echocardiography performed on conscious animals under light anesthesia (1.5% isoflurane by nose cone inhalation). Echocardiography was followed by survival surgery in all MFS mice. In preparation for surgery, mice were anesthetized using 2.5% isoflurane introduced via nose cone and 2% isoflurane for endotracheal anesthesia maintenance during the thoracotomy procedure.

Before surgery, 2 slow-release preparations based on poly lactic-co-glycolic acid (PLGA; Sigma-Aldrich) were prepared to obtain PLGA eluting films with or without the addition of a leptin antagonist[22] (LepA; superactive mouse LepA; PLR Rehovot Israel). We used PLGA 65:35 (P2066) matrix designed for slow release over 6 weeks, and PLGA 75:25 (P1941) suitable for extended release over 3 to 6 months. LepA is a mutated version of the leptin hormone with a 60-fold higher affinity for leptin receptor compared with native leptin. When applied at the aortic root wall, LepA presumably occupies most local leptin receptors, whereas native leptin remains unbound, and the pathway is rendered inactive. The surgical procedure included left thoracotomy performed through the third intercostal space to allow exposure of the proximal ascending aorta. Two miniature (1×1.5-mm) PLGA slow-release films (one P2066 and one P1941) were applied to the anterior surface of the aortic root/ascending aorta. Eleven MFS mice received both types of PLGA LepA eluting films, each containing 5 µg LepA (10 µg total) (referred to as LepA-treated MFS mice), whereas in another group of 10 MFS mice, each received similar 2 PLGA films that were devoid of LepA (referred as MFS mice), and were applied at the same location. The thoracotomy wound was closed with a 5-0 Ethicon stitch. Animals were placed on a circulating water heating pad and subcutaneous fluids were given to prevent hypothermia and dehydration, respectively. Heart rate and body temperature were monitored continuously during the surgical procedure and following surgery. Monitoring continued after the removal of the endotracheal tube, and the animals were returned to regular housing once they displayed full alertness, normal respiration, no hemorrhage, and no hypothermia.

Postoperatively, animals received analgesia, buprenorphine, SC, 0.05 to 0.1 mg/kg, and ketoprofen, SC, 1 to 2 mg/kg, every 12 hours, for the first 48 to 72 hours. The animals were monitored daily throughout the study at a designated housing facility in Brigham and Women's Hospital. Perioperative death occurred in 2 mice because of anesthetic complications. Thus, 21 MFS mice (10 MFS and 11 LepA-treated MFS mice) recovered from surgery and were followed up for 30 days. Mice were euthanized by inhaling an isoflurane overdose. Blood was flushed from the heart and aorta by injecting PBS (pH 7.4) into the left ventricle, and draining the liquid through the incised right auricle. This was followed by perfusion fixation with 4% paraformaldehyde. The heart, lungs, and proximal aorta were excised for further fixation in 10% formalin for 24 hours.

Echocardiography

All mice underwent echocardiography at baseline (21 MFS and 4 WT mice). Longitudinal echocardiography scans were performed at designated time points (2-week assessment for randomly selected 5 MFS and 5 LepA-treated MFS mice; and for all mice at 4 weeks). The images captured over time were analyzed using Vevolab proprietary software. A combination of structural and functional ultrasound imaging was performed in vivo in all MFS mice and their WT littermates by a single imager. The probes used for imaging ranged from MX550S to MX400, providing high-resolution image acquisition of the aorta and the heart, at high frame rates. Color-Doppler and pulsed-wave modalities were used to assess the peak velocities at the level of the aortic outflow tract. The Vevolab proprietary software–based analysis

package was then used to measure the diameter of the aortic root and MPA, as well as the dimensions of the left ventricle, to assess systolic function. The maximal vessel diameter was measured from B-mode analyses. Each examination included 3 measurements obtained at the level of Valsalva sinuses. The left ventricular (LV) systolic parameters were recorded in mildly sedated mice (maintained heart rate of ≈500 beats per minute), and later calculated from the short-axis M-mode images acquired at the mid papillary level. LV parameters included fractional shortening percentage, fractional area change percentage, ejection fraction percentage, end diastolic diameter, and end systolic diameter. LV mass was calculated from measured echocardiography parameters. All cardiac functional measurements were averaged over 3 consecutive cycles. Aortic valve regurgitant flow and outflow were visualized at the same angle for every animal, and color-Doppler allowed differentiation of inflow. The degree of aortic regurgitation (AR) was determined by the peaks captured in the color-Doppler mode. Echocardiography studies were evaluated by 2 experienced echocardiography scientists who were blinded to the treatment each mouse had received.

Blood Pressure Measurements

Systolic blood pressure was measured via tail cuff, using the BP-2000 Series II blood pressure analysis system (Visitech Systems). Measurements were performed in 5 randomly selected MFS mice at baseline before surgery and in 8 MFS mice from each group, 30 days postoperatively (POD30). Mice were trained on the BP system 3 times before recording of baseline systolic blood pressure. Two measurements were taken per mouse at every round, where each assessment consisted of 40 measurements, lasting 1 minute. The first 10 measurements were discarded. Outliers were excluded using Chauvenet's criterion. Notably, our analyses were focused only on recorded systolic blood pressure, as diastolic measurements are inherently inaccurate using tail cuff method.[23] Although blood pressure was not measured in WT mice, multiple reports in the literature indicate that 7- to 11-week-old C/57 WT mice are normotensive.[24]

Histology

Histochemical analysis was performed on 5-μm thick paraffin slides prepared from cross-section of aortic root and LV fixed tissues. Slides were stained with Verhoeff–van Gieson stain and Masson trichrome.

Immunohistochemistry

Paraffin slides were treated with antigen retrieve solution (DAKO), pH 9.0, for 20 minutes, followed by 3% H_2O_2 for 20 minutes, and blocking with avidin and biotin (Vector Labs) and finally R.T.U block (Vector Labs). Primary antibody against leptin (R&D Systems, catalog No. AF498) was diluted 1:80 in R.T.U block and incubated with the slides overnight. A rabbit anti-goat IgG (1:200 dilution) was used as the secondary antibody (Vector Labs). Primary antibody against TGFβ1 (Abcam, catalog No. ab215715) was used at a dilution of 1:200. A goat anti-rabbit IgG 1:200 dilution was used as a secondary antibody (Vector Labs). Staining was developed by using LSAB 2 (DAKO) and Nova Red chromogen (Vector Labs). Nonimmune IgG was used for negative control.

The following immunohistochemistry analyses were performed on the Leica Bond automated staining platform. Antibody to pSmad2 from Cell Signaling Technologies (catalog No. 3104, clone Ser245/250/255) was run at 1:1000 dilution using the Leica Biosystems Refine Detection Kit with citrate antigen retrieval. Antibody Mac-2 from Cedarlane (catalog No. CL8942AP, clone M3/38) was used at 1:8000 dilution using the Leica Biosystems Refine Detection Kit with citrate antigen retrieval. Antibody angiotensin-converting enzyme 1 (ACE-1) from Abcam (catalog No. ab75762, clone EPR2757) was used at 1:500 dilution using the Leica Biosystems Refine Detection Kit with EDTA antigen retrieval. Antibody angiotensin-converting enzyme 2 (ACE-2) from Abcam (catalog No. ab108252, clone EPR44352) was used at 1:200 dilution

Figure 1. Local application of leptin antagonist (LepA) inhibits medial degeneration.
Histological characterization of aortic root wall in Marfan syndrome (MFS) mice (30 days postoperatively for MFS and LepA-treated MFS mice, 11 weeks for all). (**A**1-3) Verhoeff–van Gieson (VVG) staining in MFS, LepA-treated MFS mice, and untreated wild-type (WT) mice. Note multiple disruptions of medial elastic fibers in MFS vs preserved elastic lamellae in LepA-treated MFS mouse, which was comparable to WT. (**B**1-3) Masson trichrome staining demonstrating depletion of smooth muscle cells and increased deposition of extracellular collagenous material in MFS (arrows) compared with LepA-treated MFS and WT untreated mice. Bars=50 μm (**A** and **B**). **C**, Number of fractures in medial elastic fibers per viewed field in aortic root from MFS, LepA-treated MFS, and WT mice. **D**, Wall thickness of aortic root from MFS, LepA-treated MFS, and WT mice. (**E**1, 2) Immunohistochemistry analysis for Mac2 in MFS and LepA-treated MFS mice. There is macrophage infiltration in the aortic root media of the MFS (white arrows), whereas the LepA-treated MFS aortic root media are devoid of inflammatory cells, with macrophages only in the perivascular tissue (black arrows). The white broken line defines the medial border. $^{**}P<0.01$, $^{***}P<0.001$. (**F**1-4) Matrix metalloproteinase 9 (MMP9) antigen was abundantly demonstrated within aortic wall and periaortic inflammatory infiltrates in MFS (1), higher magnification (2), absent in WT mice (3), and rarely evident in LepA-treated MFS mice (4).

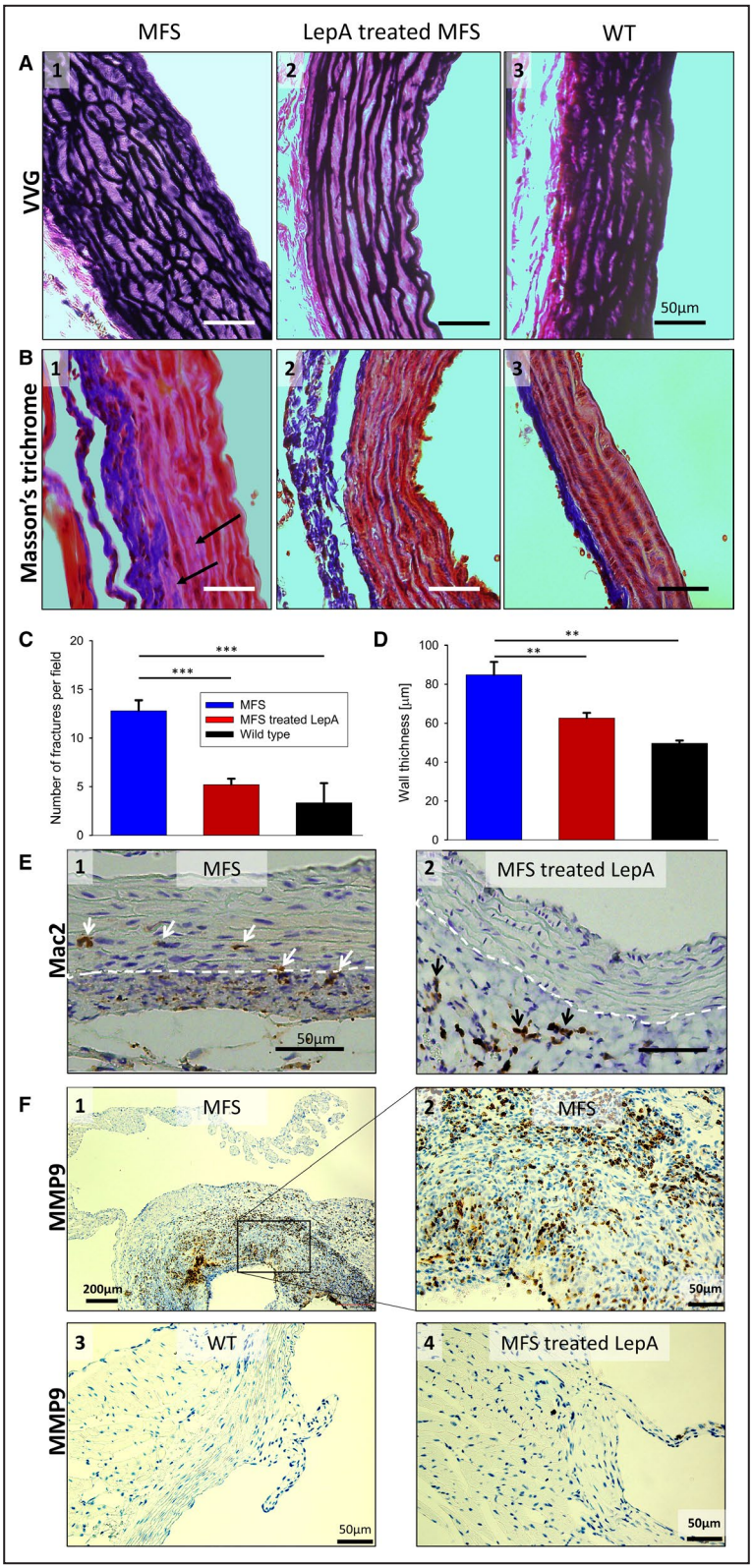

using the Leica Biosystems Refine Detection Kit with EDTA antigen retrieval. Antibody AGTR1 from Sigma (catalog No. 3500209, polyclonal) was used at 1:100 dilution, and anti-MMP9 antibody (4a3) (nbp2-13173) from Novus Biologicals, 1:100, was used with the Leica Biosystems Refine Detection Kit with EDTA antigen retrieval. In all immunohistochemistry assays, experimental groups were blinded to analysts.

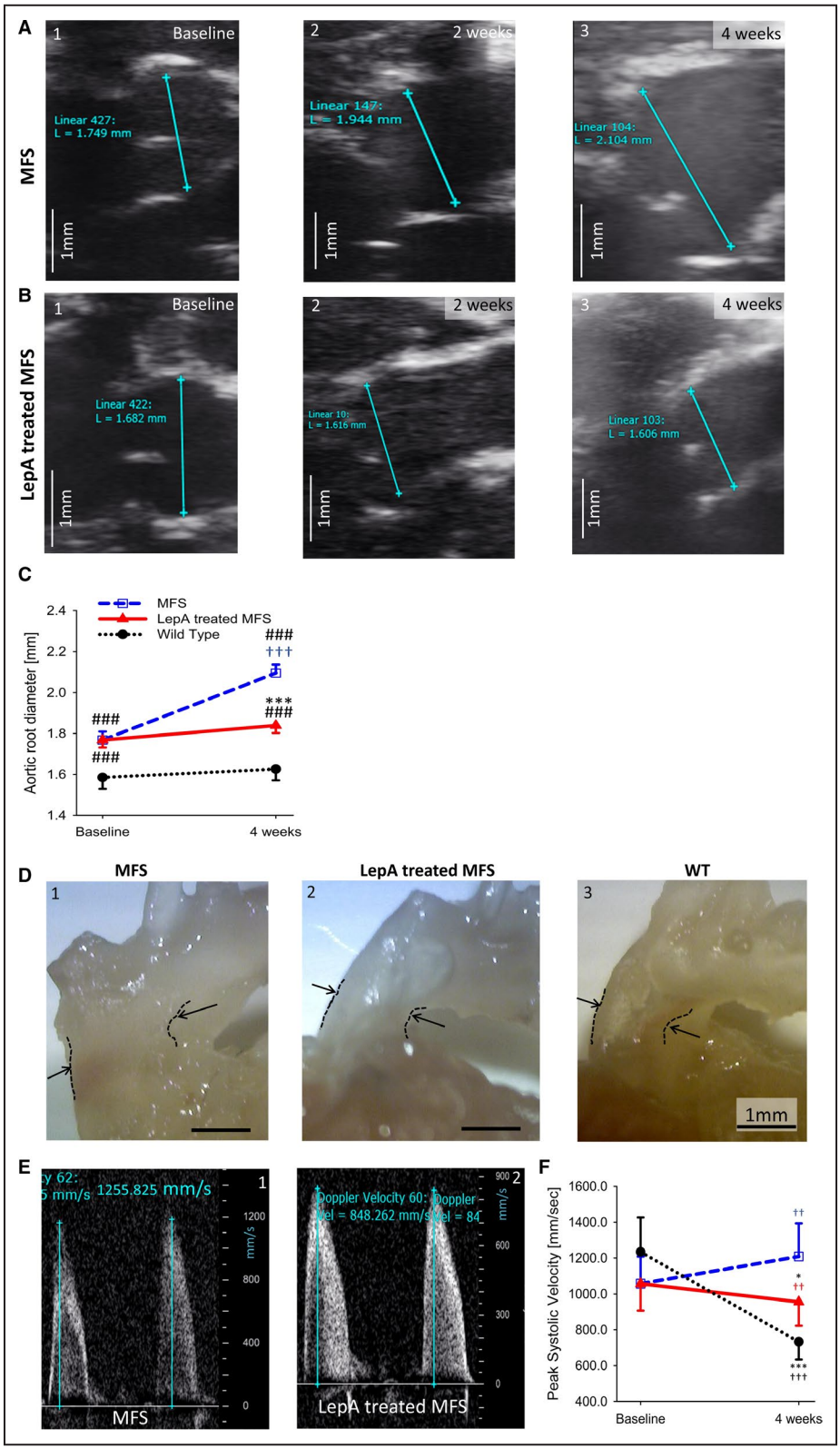

In total, 10 saline-treated MFS and 11 LepA-treated MFS aortic samples were analyzed. Additional 4 WT aortic samples from littermate siblings were used to establish background baseline. Each aortic sample underwent 8 to 10 serial sections for histochemistry, and representative histological results are shown for the various staining treatments.

Histological slides were examined at ×20 and ×40 magnification using Olympus microscope BX51. Immunohistochemistry slides were reviewed by 2

Figure 2. Aortic root dimensions in Marfan syndrome (MFS), leptin antagonist (LepA)–treated MFS mice, and wild-type (WT) mice.

B-mode view of aortic root, at the level of Valsalva sinus in MFS mice, after periaortic application of empty film (saline-treated MFS) or LepA-loaded (LepA-treated MFS) poly lactic-co-glycolic acid (PLGA) films. **A**, Empty (saline-treated MFS) PLGA films applied in MFS mice. Aortic root diameter (mm) at baseline (7 weeks), 2 weeks (9 weeks), and 30 days postoperatively (POD30) (11 weeks) (**A**1-3). **B**, LepA-loaded PLGA film in LepA-treated MFS. Aortic root diameter at baseline, 2 weeks later, and 4 weeks (POD30, 11 weeks) (**B**1-3). **C**, Aortic root diameter at baseline and after 4 weeks in untreated WT mice (black), MFS (blue), and LepA-treated MFS mice (red) (LepA-treated MFS vs MFS on POD30 ***P<0.001). **D**, Gross morphological features of aortic root in MFS, LepA-treated MFS, and WT mice displaying difference in outside diameter on POD30 (11 weeks). Bar=1 mm. **E**, Peak systolic velocity (PSV; (mm/s) in the left ventricular outlet in MFS and LepA-treated MFS mice, measured on POD30 (**E**1, 2). **F**, PSV (mm/s) at baseline and after 4 weeks in MFS, LepA-treated MFS, and untreated WT mice. *P<0.05, LepA-treated MFS vs MFS on POD30; ***P<0.001, LepA-treated MFS or WT vs MFS on POD30; ††P<0.01 vs baseline; †††P<0.001 vs baseline; ###P<0.001 vs WT.

independent observers, blinded to the treatment each mouse had received. A total of 6 to 10 regions of interest per slide were examined, all of which were representative of the entire section.

Immunohistochemistry signal intensity of leptin, ACE-1, ACE-2, and AT1R in the aortic root, as well as ACE-1, ACE-2, and AT1R in the myocardium was quantified by a custom-built Python script, expressed as percentage of positive pixels.

Leptin antigen intensity in the myocardium was assessed by ImageJ version 2.0.0-rc-68/1.52e. The latter was also used to measure cardiomyocyte cross-sectional area. To avoid misreading, this analysis was performed on selected cells that were visualized with a centered nucleus.

Analysis of Aortic Root Wall Architecture

The aortic root wall was assessed in all mice for number of fractured medial elastin fibers and wall thickness, per viewing field. Ten different representative fields per slide from at least 8 mice from each MFS group and 4 WT mice were viewed. All histological examinations were performed by 2 independent observers, blinded to the treatment each mouse had received.

Statistical Analysis

All results are presented as mean±SE. Parameters were analyzed with 2-way ANOVA with repeated measurements, in which the group (WT, MFS, and LepA-treated MFS) and time (baseline and 4 weeks) were the independent variables. One-way ANOVA was used when measurements were taken at a single time point, and the group (WT, MFS, and LepA-treated MFS) was the independent variable. Because the WT group consisted of only 4 animals, making the assumption of normal distribution void, ANOVA on ranks was used to analyze the data. The Holm-Sidak test was used as post hoc test, whenever a significant difference was found by ANOVA. Analysis was performed by SigmaStat for Windows version 3.11 (Systat Software, Inc, San Jose, CA). The Mann-Whitney U test was used to evaluate the significance of differences between MFS (saline-treated group) versus LepA-treated group. P<0.05 was considered statistically significant.

RESULTS

Experimental Animals and Treatments

The *Fbn1*$^{C1039G/+}$ heterozygous mice that were used in the current study presented typical features of MFS, including kyphoscoliosis of the vertebral column (Figure S1A and S1B) and lung and peripheral air space widening (Figure S1C1, C2). WT littermates exhibited normal skeletal structure and lung histology (Figure S1C3). More important, MFS mice treated locally with a periaortic PLGA patch eluting LepA (LepA-treated MFS), or without LepA (MFS), gained weight at a rate similar to WT mice (Figure S1D). Local LepA application did not impact the (skeletal) vertebral column or pulmonary structural manifestations within 30 days of follow-up, thereby suggesting the absence of systemic effects.

LepA Application Prevents Medial Degeneration of the Aortic Root in MFS Mice

At POD30, we demonstrated advanced medial degeneration in aortic roots of MFS versus LepA-treated MFS mice or unoperated WT (Figure 1A and 1B). MFS mice exhibited significantly more fragmentation of medial elastic fibers (P<0.001; Figure 1C), depletion of SMCs, abundance of collagenous extracellular material (arrows), and increased aortic wall thickness (P<0.01; Figure 1D). In contrast, LepA-treated MFS mice exhibited preserved histological integrity of the aortic root, resembling the histological features in WT mice. Infiltrating macrophages observed in the media and adventitia of MFS mice were absent in the media of LepA-treated MFS mice (Figure 1E1, 2), confirming a local anti-inflammatory effect of leptin inhibition. Immunohistochemistry analysis revealed abundance of MMP-9 signal within medial and adventitia invaded by inflammatory infiltration in the aortic root of MFS mice (Figure 1F1, 2). MMP-9 signal was rare in LepA-treated MFS (Figure 1F4) and completely absent in WT samples (Figure 1F3).

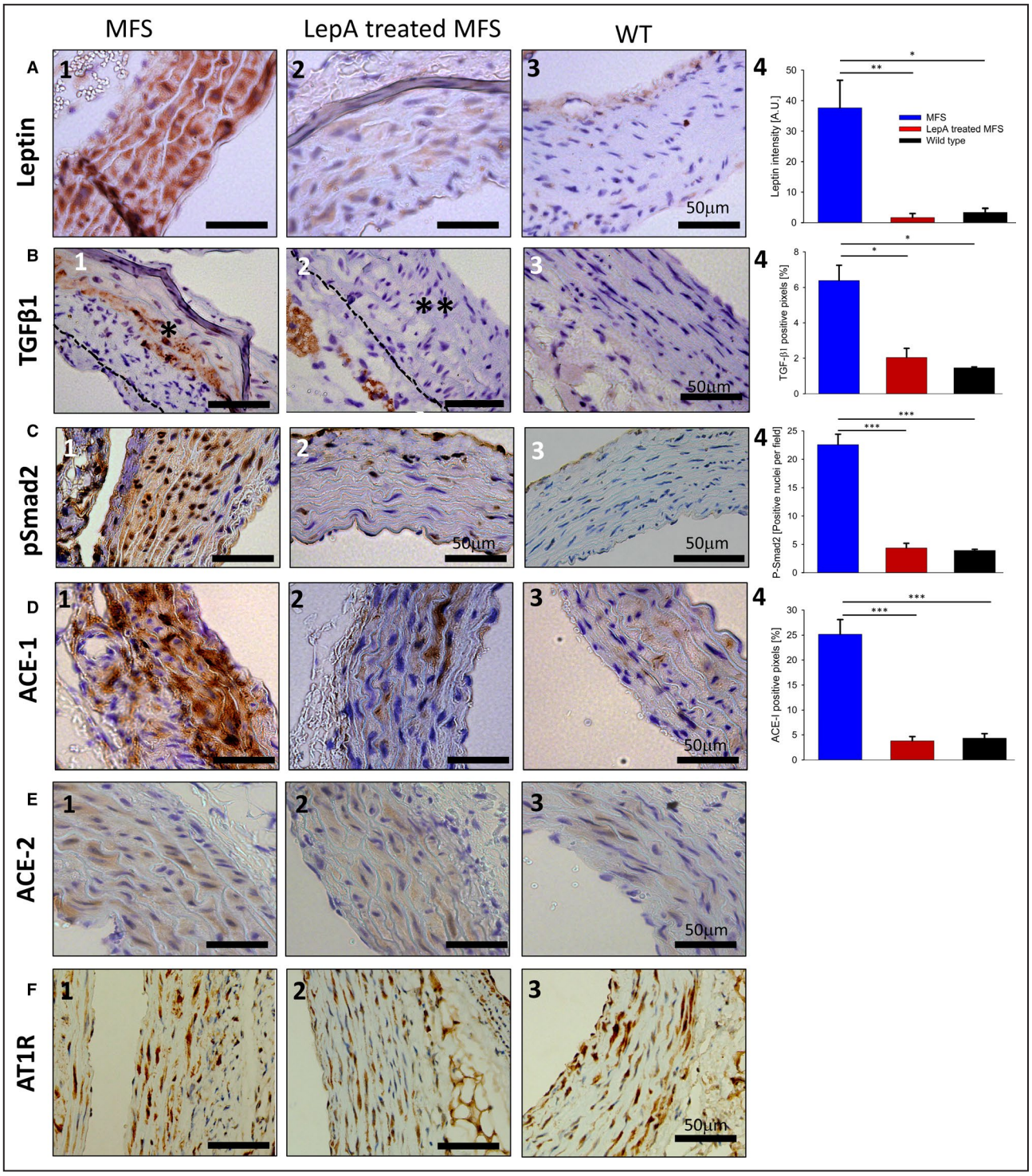

Periaortic Application of LepA Inhibited Aortic Root Expansion in MFS Mice and Preserved Hemodynamic Parameters at the LV Outlet

Baseline echocardiography of the aortic root at the level of Valsalva sinus performed in 7-week-old MFS mice revealed a larger diameter than in littermate WT mice (1.78±0.02 versus 1.59±0.07 mm, respectively). Echocardiography demonstrated that the aortic root diameter in MFS mice was already increased after 2 weeks and grew further to reach a 22% difference compared with baseline diameter after 4 weeks (2.17±0.04 mm; $P<0.001$; Figure 2A1-3). In contrast, the aortic root diameter was preserved in LepA-treated MFS mice within the same time frame (1.84±0.04 mm; Figure 2B1-3), as

Figure 3. Angiotensin II (AngII) generation and activation in aortic root wall of Marfan syndrome (MFS) mice.
Representative results of immunohistochemistry analysis of aortic root from MFS, leptin antagonist (LepA)–treated MFS (30 days postoperatively), and untreated wild-type (WT) mice (11 weeks). **A**, Leptin (brown staining): Note high expression in MFS (1), downregulated in LepA-treated MFS (2) mice, comparable to WT (3). Bar=50 μm. MFS vs LepA-treated MFS and WT (percentage positive pixels), ** and *, $P<0.01$ and $P<0.05$, respectively (4). **B**, Transforming growth factor (TGF) β1 (brown staining): Note abundant expression in the media of MFS (*) (1), vs absence of medial signal in LepA-treated MFS mice (**) (2), and scarcely evident in WT (3). Note line defining the medial border. Bar=50 μm. MFS vs LepA-treated MFS and WT (percentage positive pixels),*, $P<0.05$, for both (4). **C**, Phosphorylated Smad2 (pSmad2; brown staining of nuclei): Note high expression represented by multiple positive nuclei in MFS (1) vs the lower signal in LepA-treated MFS (2) and WT (3) mice. Bar=50 μm. MFS vs LepA-treated MFS and WT (positive nuclei per field), ***, $P<0.001$, for both (4). **D**, Angiotensin-converting enzyme 1 (ACE-1) (brown staining): Note abundance of ACE-1 protein in MFS (1), whereas LepA-treated MFS (2) and WT mice (3) exhibit a faint signal. Bar=50 μm. MFS vs LepA-treated MFS and WT(percentage positive pixels), ***, $P<0.001$, for both (4). **E**, Angiotensin-converting enzyme 2 (ACE-2) (brown staining): Note equally low signal in aortic root of MFS (1), LepA-treated MFS (2), and WT mice (3). Bar=50 μm. Quantified ACE-2 signal was similar in MFS and LepA-treated MFS mice. **F**, AngII type 1 receptor (AT1R) (brown staining): An equal signal in MFS (1), LepA-treated MFS (2), and WT mice (3). Bar=50 μm. Quantified AT1R signal was similar in MFS and LepA-treated MFS mice. A.U. indicates arbitrary unit.

well as in WT mice (1.63±0.07 versus 1.59±0.07 mm). Thus, the aortic root diameter at 4 weeks in MFS was significantly larger than in LepA-treated MFS mice ($P<0.001$; Figure 2C). Echocardiographic measurements of the luminal diameter of the aortic root were in agreement with the gross morphological features of the same segment (Figure 2D1-3). Peak systolic velocity was increased in MFS mice at POD30 compared with baseline ($P<0.01$), and decreased in LepA-treated MFS mice ($P<0.01$), to give a significant difference between LepA-treated MFS and MFS mice at 4 weeks ($P<0.05$; Figure 2E1, 2, and 2F).

Echocardiography revealed no AR in MFS mice at 7 weeks old, but 4 weeks later, a mild to moderate AR (grade 1–3) could be seen in 80% of MFS, whereas MFS mice receiving periaortic LepA treatment exhibited 73% AR, indicating insignificant difference. The presence or severity of AR did not correlate with the aortic root diameter in MFS mice. In addition, no AR could be demonstrated in the WT mice at any time during the experiment.

Activated AngII Signaling Drives Aortic Root Dilatation

By POD30, leptin, a key mediator of AngII activity, was abundantly expressed in aortic root samples from MFS mice, whereas LepA-treated MFS and WT mice exhibited low leptin expression (Figure 3A1-3; $P<0.01$ and $P<0.05$, respectively). These findings support our hypothesis that leptin is excessively expressed in the MFS-associated aneurysm wall, and suggest a causal relationship with the observed medial degeneration. As anticipated, MFS mice exhibited high levels of TGFβ1 and increased pSmad2 nuclear signal, indicative of activated TGFβ1 signaling in the aortic root media. In contrast, media from LepA-treated MFS, as well as WT mice, were both devoid of this TGFβ1 signal (Figure 3B1-3; $P<0.05$), and only a few pSmad2-positive nuclei were identified (Figure 3C1-3; $P<0.001$). To investigate AngII generation, we assessed the levels of the ACE-1 and ACE-2 antigen in the aortic root. Immunohistochemical analysis revealed upregulated ACE-1 expression in MFS mice versus low expression in LepA-treated MFS and WT mice (Figure 3D1-3; $P<0.001$, for both). Thus, decreased ACE-1 synthesis contributing to local attenuation of AngII signaling may account for reduced local leptin expression. A low signal of ACE-2 expression was evident in the aortic roots of mice in both treatment groups (Figure 3E1-3). Collectively, immunohistochemistry results suggested enhanced AngII synthesis, supporting its augmented activity in the aortic root. Interestingly, AT1R, which is involved in most AngII signaling activities in vascular SMCs and the heart, was equally expressed in all groups of mice (MFS, LepA-treated MFS, and WT; Figure 3F1-3).

Periaortic Application of LepA Inhibited Dilatation of the Adjacent MPA in MFS Mice

LepA applied to the surface of the aortic root in MFS mice was also attached to the adjacent MPA, thereby spreading LepA through diffusion from the PLGA film. Echocardiography on POD30 (Figure 4A1, 2 and 4B) showed an increase in MPA diameter from baseline in MFS mice (1.60±0.04 versus 1.47±0.04 mm at baseline) but not in LepA-treated MFS animals (1.38±0.04 after 4 weeks versus 1.43±0.04 mm at baseline). Histological features of MPA samples from MFS mice exhibited features of medial degeneration (namely, disruption of medial elastic fibers, depletion of SMCs, and abundance of ECM) (Figure 4C1) versus samples from LepA-treated and WT mice (Figure 4C2, 3). Also, abundant pSmad2-positive nuclei were evident in MPA samples from MFS mice, but rarely found in samples from LepA-treated MFS or WT mice (Figure 4D1-3). These findings imply that MFS-related medial degeneration in the MPA is driven by similar mechanisms to those proposed for the aortic root. The effect of LepA preserving MPA wall integrity may indicate its capacity to inhibit the expansion of any blood vessel, subjected to leptin-driven medial degeneration.

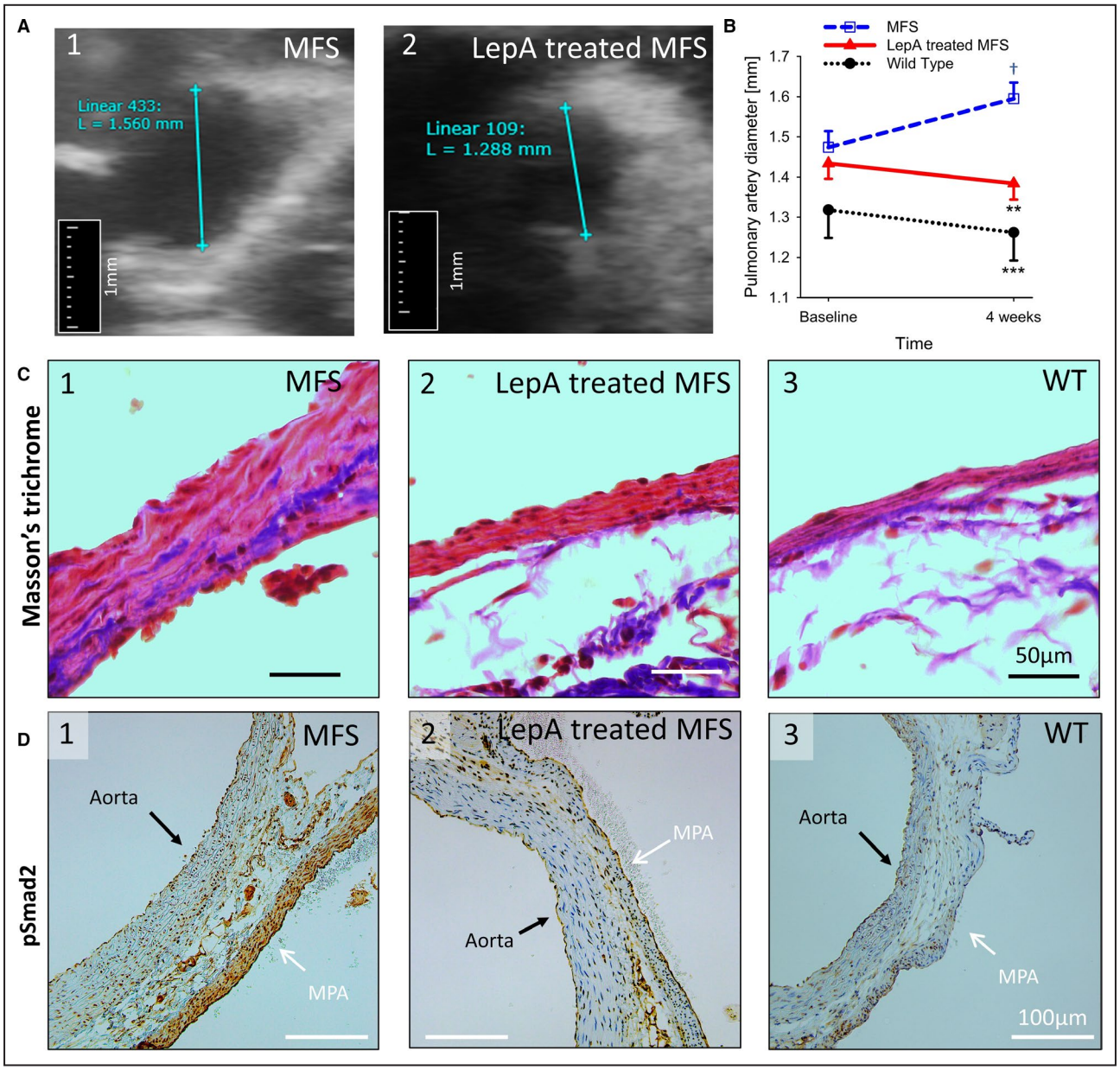

Figure 4. Effects of periaortic leptin antagonist (LepA) application on main pulmonary artery (MPA) diameter and wall histological features.

A, B-mode view of MPA in Marfan syndrome (MFS) (1) and LepA-treated MFS (2) mice at 30 days postoperatively (POD30). Note preserved vessel diameter in LepA-treated MFS (see Results). **B**, MPA diameter at baseline in MFS, LepA-treated MFS on POD30, and wild-type (WT) mice (11 weeks). Note, MFS vs LepA-treated MFS and vs WT, **, $P<0.01$ and ***, $P<0.001$, † $P<0.05$, vs. baseline; respectively. **C**, Masson's trichrome staining of MPA wall on POD30 in MFS (1), LepA-treated MFS (2), and untreated WT mice (age 11 weeks) (3). Bar=50 µm. **D**, Immunohistochemistry staining for pSmad2 on POD30 in MFS (1), LepA-treated MFS mice (2), and unoperated WT mice (11 weeks). Note reduced pSmad2 nuclear signal in MPA wall of LepA-treated MFS as well as in WT mice (white arrow). A similar pattern was observed in the adjacent aorta (black arrow). Bar=100 µm.

LepA Application at the Aortic Root of MFS Mice Was Associated With Preservation of LV Systolic Function

Baseline assessment of LV dimensions and systolic function at 7 weeks of age included measurement of the LV end diastolic diameter, end systolic diameter, fractional shortening percentage, fractional area change percentage, and ejection fraction percentage. All these parameters in MFS mice were found to be within the normal range obtained from WT sibling mice. Echocardiography performed 4 weeks later (at age 11 weeks) showed that the end diastolic diameter had increased in LepA-treated

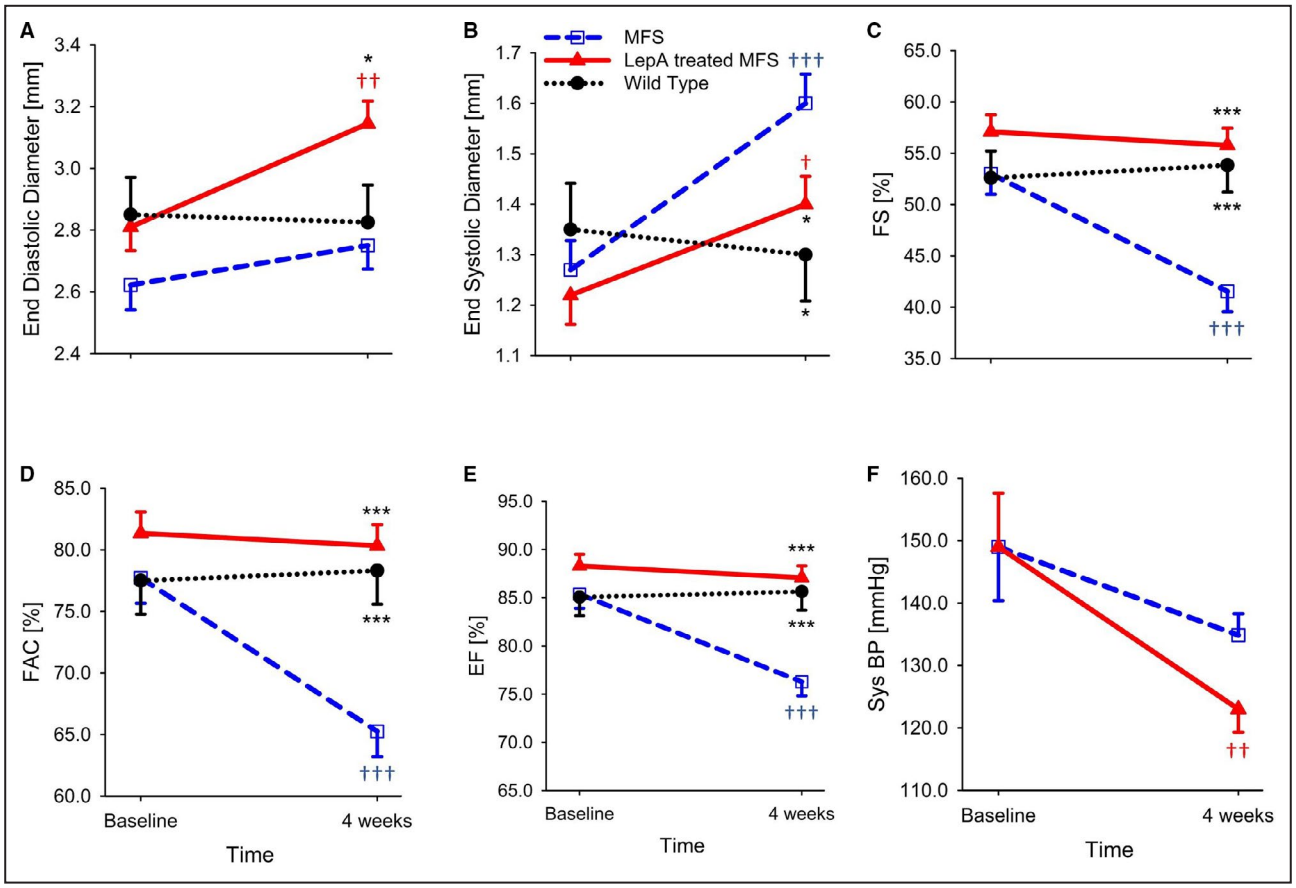

Figure 5. Effects of periaortic leptin antagonist (LepA) application on left ventricular (LV) systolic function and morphological features.

Echocardiographic assessment of LV dimensions at baseline (7 weeks) and after 4 weeks at 30 days postoperatively (POD30). **A**, End diastolic diameter (EDD). Note, EDD assessed 4 weeks postoperatively was increased in LepA-treated Marfan syndrome (MFS) vs baseline and MFS, ††, $P<0.01$ and *$P<0.05$, respectively. **B**, End systolic diameter (ESD). Note, ESD increased in MFS mice on POD30 compared with baseline and wild type (WT) at 4 weeks, ††† $P<0.001$ and *$P<0.05$, respectively. There was a moderate ESD increase in LepA-treated MFS mice vs baseline and vs MFS, † and *, $P<0.05$, for both. **C**, Fractional shortening (FS) percentage. Note that FS percentage in LepA-treated MFS animals remained comparable to that in WT mice, but decreased in MFS mice (††† and ***, $P<0.001$ vs baseline and MFS, respectively). **D**, Fractional area change (FAC) percentage. On POD30, FAC percentage remained stable in LepA-treated MFS and WT mice (11 weeks), but was markedly decreased in MFS mice. LepA-treated MFS, WT, and basal MFS vs 4 weeks MFS †††, $P<0.001$ vs Baseline, ***, $P<0.001$ vs MFS **E**, Ejection fraction (EF) percentage. Note that 4 weeks postoperatively, EF percentage remained stable in LepA-treated MFS and untreated WT mice, but was markedly decreased in MFS mice. LepA-treated MFS, WT, and basal MFS vs MFS on POD30, †††, $P<0.001$ vs Baseline, ***, $P<0.001$ vs MFS. **F**, Systolic blood pressure (Sys BP). Note, LepA-treated MFS mice exhibit normalization of Sys BP compared with MFS animals on POD30, ††, $P<0.01$. BP was not measured in WT mice.

MFS mice ($P<0.01$; Figure 5A), whereas end systolic diameter was moderately increased, although within the normal range for WT baseline. MFS mice exhibited no change in end diastolic diameter, but presented a highly significant increase in end systolic diameter ($P<0.001$; Figure 5B), suggestive of LV failure. Systolic dysfunction in MFS mice at 11 weeks of age presented a reduction in the values for fractional shortening, fractional area change, and ejection fraction percentages ($P<0.001$, for all), compared with their own baseline and with LepA-treated MFS mice (Figure 5C through 5E). In addition, systolic hypertension, observed in 7-week-old MFS mice at baseline (149±4 mm Hg) persisted in MFS mice (n=8; 134±4 mm Hg), but was normalized in LepA-treated MFS mice (n=8; 123±4 mm Hg; $P<0.05$) at 11 weeks of age (Figure 5F).

LepA Application at the Aortic Root Attenuates LV Hypertrophy

MFS mice presented with hypertrophy of LV cardiomyocytes ($P<0.001$), and increased ΔLV mass (LV mass at 11 weeks versus 7 weeks; $P<0.05$), compared with their LepA-treated MFS counterparts (Figure 6A through 6D). Immunohistochemistry analysis revealed that leptin and ACE-1 expression were lower in LepA-treated MFS than in saline-treated MFS mice

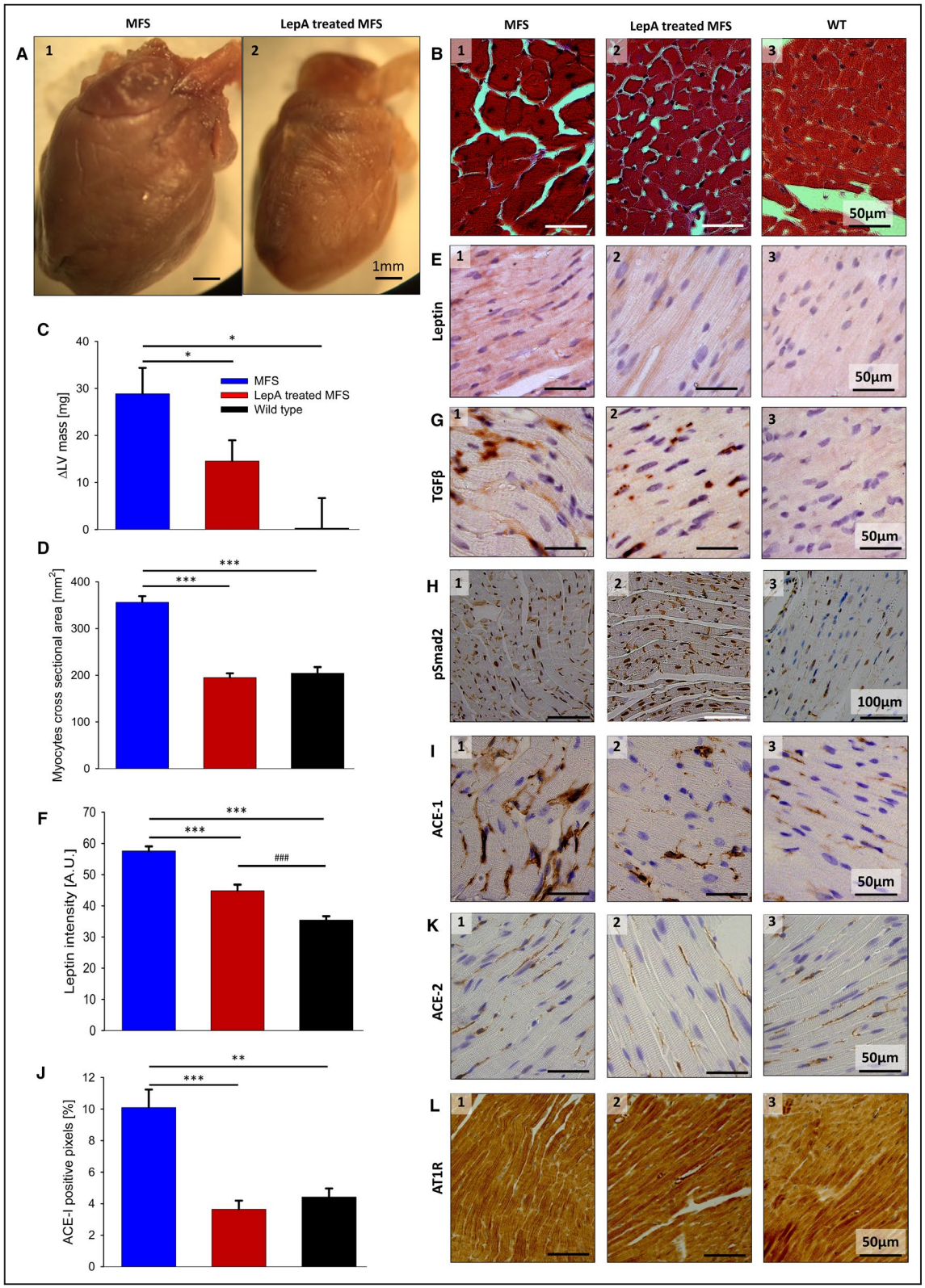

(Figure 6E and 6I). The cytoplasmatic TGFβ1 signal was scattered randomly through the LV myocardium in both MFS and LepA-treated MFS mice, without evidence of preferential expression (Figure 6G). In addition, LepA treatment in MFS mice did not affect the prevalence of pSmad2-positive nuclei (Figure 6H, Figure S2A). LepA treatment did not affect ACE-2 expression, demonstrating a weak signal in both treatment groups (Figure 6K, Figure S2B). AT1R antigen

Figure 6. Left ventricular (LV) hypertrophy; immunohistochemistry (IHC) analysis of functional effectors in the LV wall (11 weeks for all, 30 days postoperatively for Marfan syndrome [MFS] and leptin antagonist [LepA]–treated MFS).
A, Representative gross morphological features of the heart from MFS (1) vs LepA-treated MFS mouse (2). Bar=1 mm. **B**, Masson trichrome staining of LV wall cross-section in MFS (1), LepA-treated MFS (2), and wild-type (WT) mice (3). Bar=50 μm. **C**, ΔLV mass (11 vs 7 week LV mass; mg). Note a decrease in LepA-treated MFS or WT vs MFS mice, **P*<0.05, for both. **D**, Cardiomyocyte cross-sectional area (mm^2). Note the difference in size between MFS and LepA-treated MFS mice, or WT, ****P*<0.001, for both (only cardiomyocytes that were displayed with a central nucleus were measured). **E**, IHC staining for leptin antigen. Note a higher leptin signal (brown color) demonstrated in MFS vs LepA-treated MFS animals or WT. Bar=50 μm. **F**, Leptin signal intensity analysis. Note, MFS vs LepA-treated MFS or WT, ****P*<0.001, for both. **G**, IHC staining for transforming growth factor (TGF) β1 antigen (brown color). Bar=50 μm. **H**, IHC staining for pSmad2 antigen. Note equally abundant positive nuclei visualized in LV from MFS and LepA-treated MFS mice. Bar=100 μm (see Figure S2A). **I**, IHC staining for angiotensin-converting enzyme 1 (ACE-1) antigen in MFS, LepA-treated MFS, and WT. Note that the membranous signal (brown color) was reduced in LepA-treated MFS vs MFS samples. Bar=50 μm. **J**, ACE-1 signal analysis (percentage of positive pixels) in MFS, LepA-treated MFS, and WT. Note, MFS vs LepA-treated MFS and WT, ****P*<0.001 and ***P*<0.01, respectively. **K**, IHC staining for angiotensin-converting enzyme 2 (ACE-2) antigen. Note a low signal similarly demonstrated in all experimental groups. Bar=50 μm (see Figure S2B). **L**, IHC staining for angiotensin II type 1 receptor (AT1R) antigen. Note a similar signal intensity (brown color) in all experimental groups. Bar=50 μm (see Figure S2C). ****P*<0.001, LepA-treated MFS vs MFS at 4 weeks; ^{+++}P<0.001 vs baseline; $^{###}P$<0.001 vs WT. ACE-I indicates angiotensin-converting enzyme inhibitor; and A.U., arbitrary unit.

was similarly expressed in LV cardiomyocytes from MFS and LepA-treated MFS mice (Figure 6L, Figure S2C).

Periaortic Application of LepA Prevented Aortic and Mitral Valve Leaflet Thickening

Eleven-week-old MFS mice exhibited thickening of aortic and mitral valve leaflets. Same age LepA-treated MFS littermates presented normal thickness of both aortic and mitral LV valve leaflets, comparable to leaflet thickness in WT sibling (Figure 7A and 7B). The difference between MFS and LepA-treated MFS mice was statistically significant (*P*<0.01 for aortic, *P*<0.05 for mitral; Figure 7C and 7D). Leaflet thickening exhibited hyperplasia and abundance of ECM, occurring mostly at the free end of the leaflet in aortic valves and randomly localized in mitral valves.

Notably, although aortic and mitral valve leaflets in LepA-treated MFS exhibited normal thickness after 4 weeks of periaortic treatment, we cannot rule out the possibility that MFS mice already had thickened valve leaflets at the initiation of the study, and LepA therapy drove regression of leaflet lesions. There were no histological data to establish the thickness of aortic or mitral valve leaflets in MFS mice at 7 weeks of age. However, LepA-treated MFS mice exhibited LV valve leaflet thickness that was similar to WT at 11 weeks of age.

DISCUSSION

Despite considerable advances in our understanding of MFS pathophysiological feature, there is no known cure and individuals living with this condition receive lifelong systemic medical therapy. Most patients with MFS also undergo prophylactic surgery at a young age to replace an expanding, dissection-prone aortic root. We have previously shown that local inhibition of leptin activity reduces the formation of ascending aortic aneurysms in a nonphysiological AngII mouse model.[16] Using an MFS mouse model, herein we demonstrate that inhibiting leptin activity specifically at the ascending aorta prevents the medial degeneration that underlies MFS aortic root expansion.

In this study, we show that the aortic root of MFS mice displays increased levels of TGFβ1 compared with WT littermates. We also report that in addition to TGFβ1, both ACE-1 and leptin levels are elevated, indicating that they may play a role in medial degeneration, preceding the development of an aortic aneurysm. We and others have previously shown that these factors are linked to AngII signaling. Therefore, our results suggest that AngII is also involved in the process, similarly to the finding that elevated ACE-1 expression and activated AngII signaling drive the development of ascending aortic aneurysm in *fibulin-4* deficient mice.[25]

Local upregulation of ACE-1 levels in the aortic root of MFS mice could be occurring via paracrine and autocrine pathways. In a similar manner to previous findings,[26] increased levels of TGFβ at the aortic root may lead to induction in ACE-1 expression, which, then in turn, promotes further AngII production. Leptin has also been shown to regulate ACE activity at the systemic level.[27] As leptin is abundant at the MFS mouse aortic root, it may also be modulating the local induction of ACE-1. Other possible drivers are leptin-induced vascular endothelial growth factor,[28,29] increased mechanical stress, and the impact of systolic hypertension on degenerated media.[30–32]

Our data suggest that LepA locally attenuates medial degeneration via several pathways. A major effect relates to the local downregulation of ACE-1 at the aortic root, which, then in turn, decreases AngII production in the region. An additional pathway involves the observed local decrease in TGFβ1 expression via Smad2 signaling, which may have prevented transformation of vascular SMCs from the contractile to the inflammatory form at the onset of aneurysm formation.[33]

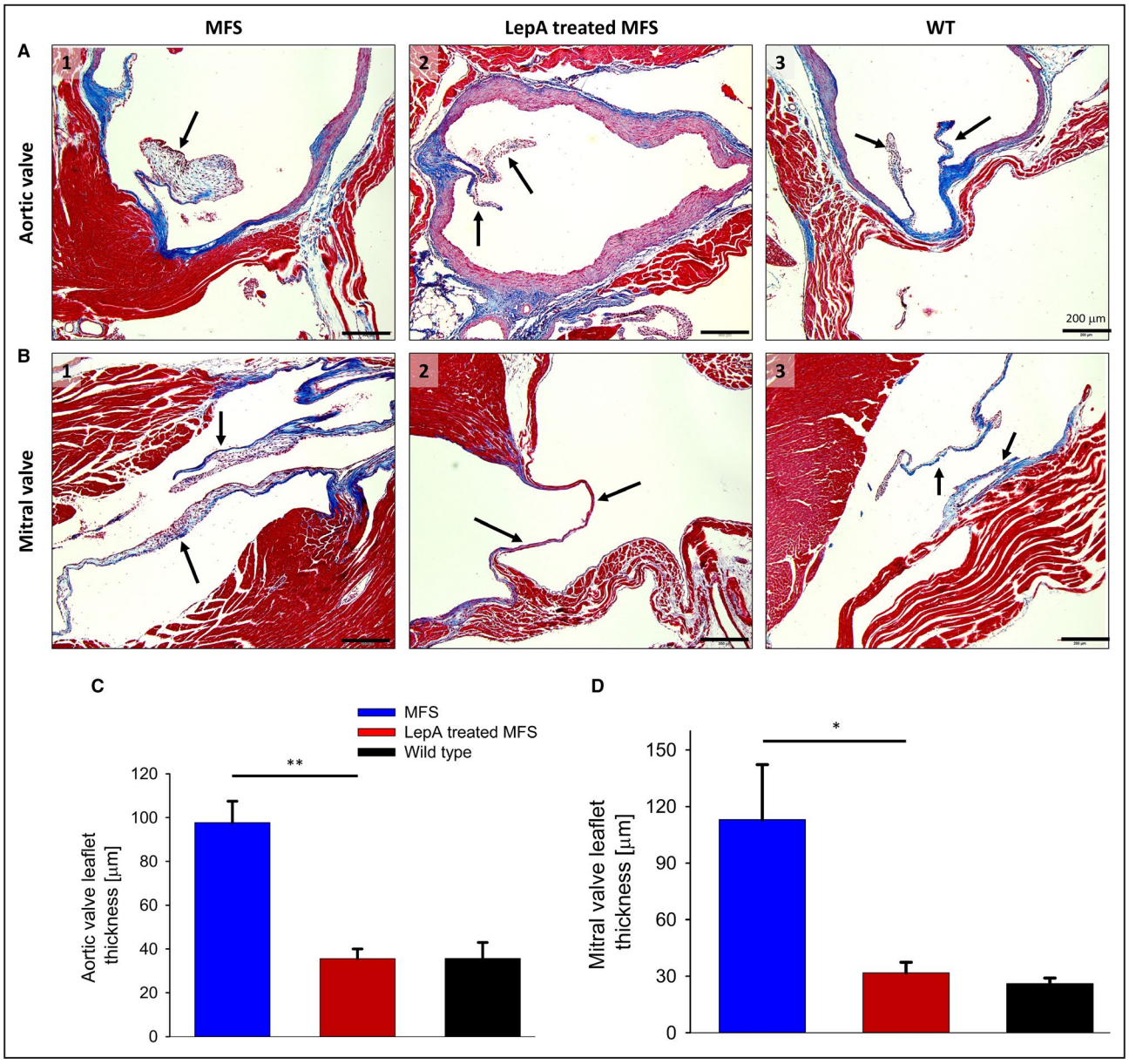

Figure 7. Local periaortic leptin antagonist (LepA) treatment prevents aortic and mitral valve leaflet thickening in Marfan syndrome (MFS) mice (30 days postoperatively [POD30]).
Representative photomicrographs of aortic and mitral valve leaflets from MFS, LepA-treated MFS, and wild-type (WT) mice at 11 weeks of age (POD30 for all MFS mice). **A**, Aortic valve leaflets from MFS (1), LepA-treated MFS (2), and WT (3) mice (arrows). **B**, Mitral valve leaflets from MFS (1), LepA-treated MFS (2), and WT (3) mice (arrows). **C**, Aortic valve leaflet thickness measured in the 3 groups. Note, MFS vs LepA-treated MFS, $^{**}P<0.01$. **D**, Mitral valve leaflet thickness measurement. Note, MFS vs LepA-treated MFS, $^{*}P<0.05$.

Local downregulation in AngII, leptin, and ACE-1 expression may also be related to decreased stress in the vessel wall. As leptin has been previously shown to locally increase reactive oxygen species production,[34] LepA treatment likely also leads to decreased local oxidative stress.

We found that local LepA treatment inhibits medial macrophage infiltration in MFS mice. This was evident from both direct staining of macrophages and immunohistochemistry analysis of MMP-9 antigen. The role of MMP-9 in MFS aortic aneurysms has been demonstrated in a different MFS mouse model.[35] Using an AngII-induced abdominal aortic aneurysm model system, we have previously shown increased MMP-9 expression, which was further augmented by the addition of periaortic leptin application.[14] Our MMP-9 results in the current study go hand in hand with our macrophage data. These findings are consistent with clinical data showing that reduced medial infiltration by macrophages is associated with downregulation of MMP activity,[36] and correlates with attenuated expansion of the aortic aneurysm.[37]

Cardiac dysfunction in patients with MFS has been attributed to several causes, including progressive insufficiency of mitral or aortic valve[38,39] and primary cardiomyopathy implicated as a consequence of *fibrillin-1* mutations.[40] Heart failure, which is the main cause of death in children with MFS, is often associated with severe mitral valve disease.[41] Although they may manifest negligible valvular pathological features, many young patients with MFS still present with dilated cardiomyopathy and LV systolic dysfunction.[42] In adults, a quarter of patients with MFS harbor an asymptomatic reduction of LV ejection fraction, resulting from impaired systolic function.[43]

Consistent with our results, heterozygous *Fbn1*$^{C1039G/+}$ mice manifest a mild degree of LV systolic dysfunction and a low tolerance for increased LV workload.[6] Although our 7-week-old MFS mice presented with normal LV function, by 11 weeks of age their systolic function had deteriorated, independent of aortic valve regurgitation presence, or unrelated to its severity. The periaortic LepA application in our model rescued LV structure and function. This was achieved by inhibiting medial degeneration and preventing expansion of the aortic root. Protected aortic integrity and preservation of its diameter played a key role in reducing the progression of LV outlet obstruction. In contrast, MFS mice underwent medial degeneration underlying aortic root dilatation, which promoted increased impedance at the LV outflow, associated with LV systolic dysfunction. Therefore, we have concluded that conserved hemodynamic conditions at the aortic outlet maintaining low LV workload were sufficient to preserve LV systolic function in *Fbn1*$^{C1039G/+}$ mice. These results are consistent with our previous findings in LepA-treated AngII-infused apolipoprotein E–deficient mice.[16]

Our current results, which underscore the importance of aortic root integrity in MFS on LV morphological features and function, may downplay the contribution of primary cardiomyopathy in driving LV dysfunction. It is likely that aortoventricular coupling decreased the intraventricular wall pressure in LepA-treated MFS mice, resulting in downregulation of AngII, leptin, and ACE-1 expression. Subsequently, decreased ACE-1 may further reduce AngII production in cardiac myocytes. Preservation of LV systolic function in LepA-treated MFS mice could be attributed, at least in part, to reduction in leptin and AngII activity, both of which promote LV systolic dysfunction.[44,45] We have found further evidence that local LepA treatment attenuates LV remodeling in MFS mice. The significant thickening of aortic and mitral valve leaflets observed in MFS mice did not occur in LepA-treated MFS mice. A similar response was revealed in LepA-treated AngII-infused apolipoprotein E–deficient mice,[16] suggesting that decreased leptin and AngII expression levels in LV cardiomyocytes play a role in attenuating LV valve remodeling.

Systolic hypertension diagnosed in 7-week-old MFS mice was corrected by 11 weeks in subjects receiving periaortic LepA. Normalization of systolic hypertension in LepA-treated MFS mice was not driven via AT1R blockage or by a systemic mechanism. Therefore, it may be attributed to reduction in cardiomyocyte AngII and leptin, as well as improvement of LV systolic function and stabilization of hemodynamic conditions in the ascending aorta. It has been suggested that the cell surface AngII type 2 receptor may drive AT1R-opposing effects by exerting vasodilatation when activated by pathological conditions of inflammation, hypertension, or acute myocardial infarction.[46] However, an AngII type 2 receptor agonist, which was tested recently in an MFS mouse model, failed to attenuate aortic root dilatation compared with losartan therapy,[47] thus suggesting that AngII type 2 receptor is likely not involved in MFS aortopathy.

Early studies in MFS mice have shown that medial degeneration involving the aortic root starts in utero.[5] Degenerative changes and rapid expansion of the aortic root in children with MFS frequently render the vessel wall vulnerable to acute type A dissection,[48] forcing many patients with MFS to undergo early prophylactic aortic replacement.[49] Medical treatment initiated at infancy or childhood frequently addresses advanced remodeling with pathological aortic root dilatation. Patients with MFS are routinely treated with β blockers, shown to reduce TGFβ expression and aortic stiffness.[50] This treatment also attenuates hemodynamic perturbations by decreasing heart rate, its oxygen consumption, myocardial contractility, and systolic blood pressure. Unfortunately, frequent adverse effects, such as hypotension and bradycardia, may necessitate alternative treatment, or require combined therapy with other agents, such as the AngII type 1 receptor blocker, losartan. Inhibiting AngII signaling through the use of AngII type 1 receptor blocker or angiotensin-converting enzyme inhibitor has been shown to attenuate medial degeneration, stabilize LV performance, and reduce blood pressure.[51] Nevertheless, the efficiency of these medications in counteracting AngII signaling pathway may be affected by the type and severity of the MFS mutation.[52] Thus, at the present time, despite strong patient compliance, currently available therapies may not provide a durable and complication-free solution for control of the cardiovascular manifestations associated with MFS.[53] There is an unmet need for a safe and effective mode of therapy that will universally inhibit aortic aneurysm formation, and prevent related cardiac complications.

In summary, this study presents evidence that local periaortic antileptin therapy can be effective

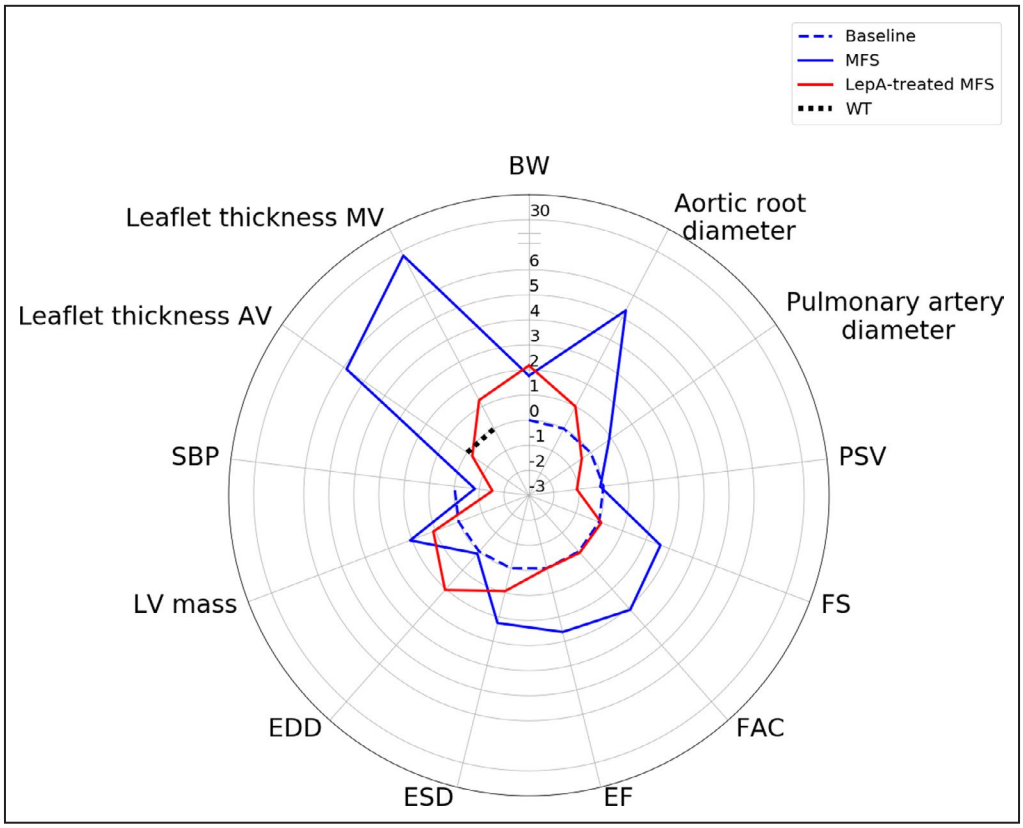

Figure 8. Radar plot of the main physiological results described in this study.
Each axis shows the standard score (number of SDs) of the mean value of leptin antagonist (LepA)–treated Marfan syndrome (MFS) (full red) and MFS (full blue) mice at 30 days postoperatively with respect to mean baseline MFS levels (dashed blue line). BW indicates body weight; EDD, end diastolic diameter; EF, ejection fraction; ESD, end systolic diameter; FAC, fractional area change; FS, fractional shortening; LV, left ventricular; PSV, peak systolic velocity; SBP, systolic blood pressure; AV, aortic valve and MV, mitral valve.

in preventing the development of aortic root aneurysm in a mouse model of MFS. We identify locally expressed leptin as a uniform culprit effector driving medial degeneration in MFS, as well as in a variety of systemic diseases. Periaortic application of LepA attenuates local leptin-driven deleterious effects and downregulates AngII signaling pathway at the site of therapy, likely via local reduction of TGFβ and ACI-1 expression. MFS aortopathy promotes local hemodynamic perturbations, and thereby increases LV workload. Pressure-induced overexpression of leptin and ACI-1 in LV cardiomyocytes drives hypertrophy and systolic dysfunction. Thus, periaortic LepA therapy preserving aortic root integrity prevents LV functional deterioration (Figure 8). Our results suggest a stand-alone local therapy that may prove to be a viable alternative to life-long systemic treatment to counteract MFS-related aortopathy, free of systemic complications. On the basis of its protective properties, we anticipate a positive therapeutic response when using local LepA application in variable aneurysms (namely, aortic, peripheral, and visceral lesions), which are driven by AngII or TGFβ signaling, including TGFβ receptor mutations.[54]

LIMITATIONS OF THIS STUDY

This study does not include the long-term follow-up (beyond 30 days) to reveal the full effects of local LepA therapy on gross morphological features, histological changes, and susceptibility to acute dissection in the aortic root, as well as its impact on related cardiac structure and function. In addition, although we demonstrated the beneficial therapeutic potential of LepA in young MFS mice, the current study does not include testing on older mice, which may respond differently with respect to the prevention of aortic root dilatation and salvaged LV function. Other limitations of the study are lack of female MFS mice in our series and unavailable data on the kinetics of locally applied LepA, which warrant a separate dedicated study.

ARTICLE INFORMATION

Received September 26, 2019; accepted April 3, 2020.

Affiliations

From the Cardiovascular Physiology Core, Department of Medicine, Brigham and Women's Hospital, Harvard Medical School, Boston, MA (S.F., R.L.); Epidemiology Unit, Rambam Health Care Center, Haifa, Israel (N.B.H.); The Cardiovascular Research Laboratory, Research institute, Galilee Medical Center, Nahariya, Israel (O.E.); CVPath Institute, Gaithersburg, MD (L.G.); Department of Developmental Biology and Cancer Research, Institute of Medical Research Israel-Canada, Hebrew University of Jerusalem–Hadassah Medical School, Jerusalem, Israel (Y.A., D.B.-Z.); Stanford University School of Medicine, Cardiovascular Institute, Stanford, CA (R.L.); and Department of Vascular Surgery, Sheba Medical Center, Sackler Faculty of Medicine, Tel Aviv University, Tel Aviv, Israel (J.S.).

Acknowledgments

We are grateful to Fred Roberts, from FujiFilm VisualSonics, Inc, for generous technical support and to Teresa Bowman, from the Specialized Histopathology Core, Brigham and Women's Hospital, Department of Pathology, Boston, MA, for dedicated histological analyses. We thank Dana-Farber/Harvard Cancer Center in Boston, MA, for the use of the Specialized Histopathology Core, which provided histological and immunohistochemistry services. Dana-Farber/Harvard Cancer Center is supported in part by a National Cancer Institute Cancer Center Support Grant NIH 5 P30 CA06516. We thank Ming Tao from the Department of Vascular and Endovascular Surgery, Brigham and Women Hospital, Boston, MA, for technical support. We also thank Jonathan I. Schneiderman, PhD, for his critical review of the manuscript.

Author contributions: Schneiderman: designed the experiments; Bachner-Henenzon, Fisch, Guo, Ertracht, Ben-Zvi, Arad, Liao, and Schneiderman: performed experiments and/or analyzed the data; Schneiderman: wrote the manuscript.

Sources of Funding

This work was funded by a private donation from Nathan Gottesdiener.

Disclosures

For purposes of this project, no author received any payment or other support from a commercial company. Dr Schneiderman is a cofounder of Remodeless CV. He is also an inventor of 2 patents. The remaining authors have no disclosures to report.

Supplementary Materials

Figures S1–S2

REFERENCES

1. Pyeritz RE. The Marfan syndrome. *Annu Rev Med*. 2000;51:481–510.
2. Neptune ER, Frischmeyer PA, Arking DE, Myers L, Bunton TE, Gayraud B, Ramirez F, Sakai LY, Dietz HC. Dysregulation of TGF-beta activation contributes to pathogenesis in Marfan syndrome. *Nat Genet*. 2003;33:407–411.
3. Robinson PN, Godfrey M. The molecular genetics of Marfan syndrome and related microfibrillopathies. *J Med Genet*. 2000;37:9–25.
4. Dale M, Fitzgerald MP, Liu Z, Meisinger T, Karpisek A, Purcell LN, Carson JS, Harding P, Lang H, Koutakis P, et al. Premature aortic smooth muscle cell differentiation contributes to matrix dysregulation in Marfan syndrome. *PLoS One*. 2017;12:e0186603.
5. Habashi JP, Judge DP, Holm TM, Cohn RD, Loeys BL, Cooper TK, Myers L, Klein EC, Liu G, Calvi C, et al. Losartan, an AT1 antagonist, prevents aortic aneurysm in a mouse model of Marfan syndrome. *Science*. 2006;312:117–121.
6. Rouf R, MacFarlane EG, Takimoto E, Chaudhary R, Nagpal V, Rainer PP, Bindman JG, Gerber EE, Bedja D, Schiefer C, et al. Nonmyocyte ERK1/2 signaling contributes to load-induced cardiomyopathy in Marfan mice. *JCI Insight*. 2017;2:e91588. Available at: https://doi.org/10.1172/jci.Insight.91588. Accessed April 30, 2020.
7. Cook JR, Clayton NP, Carta L, Galatioto J, Chiu E, Smaldone S, Nelson CA, Cheng SH, Wentworth BM, Ramirez F. Dimorphic effects of transforming growth factor-beta signaling during aortic aneurysm progression in mice suggest a combinatorial therapy for Marfan syndrome. *Arterioscler Thromb Vasc Biol*. 2015;35:911–917.
8. Wei H, Hu JH, Angelov SN, Fox K, Yan J, Enstrom R, Smith A, Dichek DA. Aortopathy in a mouse model of Marfan syndrome is not mediated by altered transforming growth factor beta signaling. *J Am Heart Assoc*. 2017;6:e004968. DOI: 10.1161/JAHA.116.004968.
9. Franken R, Radonic T, den Hartog AW, Groenink M, Pals G, van Eijk M, Lutter R, Mulder BJM, Zwinderman AH, de Waard V, et al. The revised role of TGF-β in aortic aneurysms in Marfan syndrome. *Neth Heart J*. 2015;23:116–121.
10. Gomez D, Al Haj Zen A, Borges LF, Phillipe M, Gutierrez PS, Jondeau G, Michel JB, Vranckx R. Syndromic and non-syndromic aneurysms of the human ascending aorta share activation of the Smad2 pathway. *J Pathol*. 2009;218:131–142.
11. Ainscough JF, Drinkhill MJ, Sedo A, Turner NA, Brooke DA, Balmforth AJ, Ball SG. Angiotensin II type-1 receptor activation in the adult heart causes blood pressure-independent hypertrophy and cardiac dysfunction. *Cardiovasc Res*. 2009;81:592–600.
12. Yu C, Jeremy RW. Angiotensin, transforming growth factor beta and aortic dilatation in Marfan syndrome: of mice and humans. *Int J Cardiol Heart Vasc*. 2018;18:71–80.
13. Kagami S, Border WA, Miller DE, Noble NA. Angiotensin II stimulates extracellular matrix protein synthesis through induction of transforming growth factor-beta expression in rat glomerular mesangial cells. *J Clin Invest*. 1994;93:2431–2437.
14. Tao M, Yu P, Nguyen BT, Mizrahi B, Savion N, Kolodgie FD, Virmani R, Hao S, Ozaki CK, Schneiderman J. Locally applied leptin induces regional aortic wall degeneration preceding aneurysm formation in apolipoprotein E-deficient mice. *Arterioscler Thromb Vasc Biol*. 2013;33:311–320.
15. Ben-Zvi D, Savion N, Kolodgie F, Simon A, Fisch S, Schafer K, Bachner-Hinenzon N, Cao X, Gertler A, Solomon G, et al. Local application of leptin antagonist attenuates angiotensin II-induced ascending aortic aneurysm and cardiac remodeling. *J Am Heart Assoc*. 2016;5:e003474. DOI: 10.1161/JAHA.116.003474.
16. Koh KK, Park SM, Quon MJ. Leptin and cardiovascular disease: response to therapeutic interventions. *Circulation*. 2008;117:3238–3249.
17. Leung JC, Chan LY, Tang SC, Chu KM, Lai KN. Leptin induces TGF-beta synthesis through functional leptin receptor expressed by human peritoneal mesothelial cell. *Kidney Int*. 2006;69:2078–2086.
18. Yamagishi SI, Edelstein D, Du XL, Kaneda Y, Guzman M, Brownlee M. Leptin induces mitochondrial superoxide production and monocyte chemoattractant protein-1 expression in aortic endothelial cells by increasing fatty acid oxidation via protein kinase A. *J Biol Chem*. 2001;276:25096–25100.
19. Gruen ML, Hao M, Piston DW, Hasty AH. Leptin requires canonical migratory signaling pathways for induction of monocyte and macrophage chemotaxis. *Am J Physiol Cell Physiol*. 2007;293:C1481–C1488.
20. Park HY, Kwon HM, Lim HJ, Hong BK, Lee JY, Park BE, Jang Y, Cho SY, Kim HS. Potential role of leptin in angiogenesis: leptin induces endothelial cell proliferation and expression of matrix metalloproteinases in vivo and in vitro. *Exp Mol Med*. 2001;33:95–102.
21. Wu D, Shen YH, Russell L, Coselli JS, LeMaire SA. Molecular mechanisms of thoracic aortic dissection. *J Surg Res*. 2013;184:907–924.
22. Shpilman M, Niv-Spector L, Katz M, Varol C, Solomon G, Ayalon-Soffer M, Boder E, Halpern Z, Elinav E, Gertler A. Development and characterization of high affinity leptins and leptin antagonists. *J Biol Chem*. 2011;286:4429–4442.
23. Feng M, Whitesall S, Zhang Y, Beibel M, D'Alecy L, DiPetrillo K. Validation of volume-pressure recording tail-cuff blood pressure measurements. *Am J Hypertens*. 2008;21:1288–1291.
24. Gros R, Van Wert R, You X, Thorin E, Husain M. Effects of age, gender, and blood pressure on myogenic responses of mesenteric arteries from C57BL/6 mice. *Am J Physiol Heart Circ Physiol*. 2002;282:H380–H388.
25. Huang J, Yamashiro Y, Papke CL, Ikeda Y, Lin Y, Patel M, Inagami T, Le VP, Wagenseil JE, Yanagisawa H. Angiotensin-converting enzyme-induced activation of local angiotensin signaling is required for ascending aortic aneurysms in fibulin-4-deficient mice. *Sci Transl Med*. 2013;5:183ra58, 1–11.
26. Petrov VV, Fagard RH, Lijnen PJ. Transforming growth factor-beta(1) induces angiotensin-converting enzyme synthesis in rat cardiac fibroblasts during their differentiation to myofibroblasts. *J Renin Angiotensin Aldosterone Syst*. 2000;1:342–352.

27. Hilzendeger AM, Morais RL, Todiras M, Plehm R, da Costa Goncalves A, Qadri F, Araujo RC, Gross V, Nakaie CR, Casarini DE, et al. Leptin regulates ACE activity in mice. *J Mol Med (Berl)*. 2010;88:899–907.
28. Yang WH, Chen JC, Hsu KH, Lin CY, Wang SW, Wang SJ, Chang YS, Tang CH. Leptin increases VEGF expression and enhances angiogenesis in human chondrosarcoma cells. *Biochim Biophys Acta*. 2014;1840:3483–3493.
29. Saijonmaa O, Nyman T, Kosonen R, Fyhrquist F. Upregulation of angiotensin-converting enzyme by vascular endothelial growth factor. *Am J Physiol Heart Circ Physiol*. 2001;280:H885–H891.
30. Ghantous CM, Kobeissy FH, Soudani N, Rahman FA, Al-Hariri M, Itani HA, Sabra R, Zeidan A. Mechanical stretch-induced vascular hypertrophy occurs through modulation of leptin synthesis-mediated ROS formation and GATA-4 nuclear translocation. *Front Pharmacol*. 2015;6:240.
31. Gosgnach W, Challah M, Coulet F, Michel JB, Battle T. Shear stress induces angiotensin converting enzyme expression in cultured smooth muscle cells: possible involvement of bFGF. *Cardiovasc Res*. 2000;45:486–492.
32. Ruwhof C, van der Laarse A. Mechanical stress-induced cardiac hypertrophy: mechanisms and signal transduction pathways. *Cardiovasc Res*. 2000;47:23–37.
33. Zhao G, Fu Y, Cai Z, Yu F, Gong Z, Dai R, Hu Y, Zeng L, Xu Q, Kong W. Unspliced XBP1 confers VSMC homeostasis and prevents aortic aneurysm formation via FoxO4 interaction. *Circ Res*. 2017;121:1331–1345.
34. Xu FP, Chen MS, Wang YZ, Yi Q, Lin SB, Chen AF, Luo JD. Leptin induces hypertrophy via endothelin-1 reactive oxygen species pathway in cultured neonatal rat cardiomyocytes. *Circulation*. 2004;110:1269–1275.
35. Xiong W, Knispel RA, Dietz HC, Raminez F, Baxter BT. Doxycycline delays aneurysm rupture in a mouse model of Marfan syndrome. *J Vasc Surg*. 2008;47:166–172.
36. Boyum J, Fellinger EK, Schmoker JD, Trombley L, McPartland K, Ittleman FP, Howard AB. Matrix metalloproteinase activity in thoracic aortic aneurysms associated with bicuspid and tricuspid aortic valves. *J Thorac Cardiovasc Surg*. 2004;127:686–691.
37. Radonic T, de Witte P, Groenink M, de Waard V, Lutter R, van Eijk M, Jansen M, Timmermans J, Kempers M, Scholte AJ, et al. Inflammation aggravates disease severity in Marfan syndrome patients. *PLoS One*. 2012;7:e32963.
38. Helder MR, Schaff HV, Dearani JA, Li Z, Stulak JM, Suri RM, Connolly HM. Management of mitral regurgitation in Marfan syndrome: outcomes of valve repair versus replacement and comparison with myxomatous mitral valve disease. *J Thorac Cardiovasc Surg*. 2014;148:1020–1024.
39. Nishimura RA, Otto CM, Bonow RO, Carabello BA, Erwin JP III, Guyton RA, O'Gara PT, Ruiz CE, Skubas NJ, Sorajja P, et al. 2014 AHA/ACC guideline for the management of patients with valvular heart disease: a report of the American College of Cardiology/American Heart Association Task Force on Practice Guidelines. *J Am Coll Cardiol*. 2014;63:e57–e185.
40. De Backer JF, Devos D, Segers P, Matthys D, Francois K, Gillebert TC, De Paepe AM, De Sutter J. Primary impairment of left ventricular function in Marfan syndrome. *Int J Cardiol*. 2006;112:353–358.
41. Morse RP, Rockenmacher S, Pyeritz RE, Sanders SP, Bieber FR, Lin A, MacLeod P, Hall B, Graham JM Jr. Diagnosis and management of infantile Marfan syndrome. *Pediatrics*. 1990;86:888–895.
42. Chatrath R, Beauchesne LM, Connolly HM, Michels VV, Driscoll DJ. Left ventricular function in the Marfan syndrome without significant valvular regurgitation. *Am J Cardiol*. 2003;91:914–916.
43. Alpendurada F, Wong J, Kiotsekoglou A, Banya W, Child A, Prasad SK, Pennell DJ, Mohiaddin RH. Evidence for Marfan cardiomyopathy. *Eur J Heart Fail*. 2010;12:1085–1091.
44. Kain D, Simon AJ, Greenberg A, Ben Zvi D, Gilburd B, Schneiderman J. Cardiac leptin overexpression in the context of acute MI and reperfusion potentiates myocardial remodeling and left ventricular dysfunction. *PLoS One*. 2018;13:e0203902.
45. Rajapurohitam V, Javadov S, Purdham DM, Kirshenbaum LA, Karmazyn M. An autocrine role for leptin in mediating the cardiomyocyte hypertrophic effects of angiotensin II and endothelin-1. *J Mol Cell Cardiol*. 2006;41:265–274.
46. Lemarie CA, Schiffrin EL. The angiotensin II type 2 receptor in cardiovascular disease. *J Renin Angiotensin Aldosterone Syst*. 2010;11:19–31.
47. Verbrugghe P, Verhoeven J, Clijsters M, Vervoort D, Schepens J, Meuris B, Herijgers P. The effect of a nonpeptide angiotensin II type 2 receptor agonist, compound 21, on aortic aneurysm growth in a mouse model of Marfan syndrome. *J Cardiovasc Pharmacol*. 2018;71:215–222.
48. de Beaufort HWL, Trimarchi S, Korach A, Di Eusanio M, Gilon D, Montgomery DG, Evangelista A, Braverman AC, Chen EP, Isselbacher EM, et al. Aortic dissection in patients with Marfan syndrome based on the IRAD data. *Ann Cardiothorac Surg*. 2017;6:633–641.
49. Treasure T, Takkenberg JJ, Pepper J. Surgical management of aortic root disease in Marfan syndrome and other congenital disorders associated with aortic root aneurysms. *Heart*. 2014;100:1571–1576.
50. Bhatt AB, Buck JS, Zuflacht JP, Milian J, Kadivar S, Gauvreau K, Singh MN, Creager MA. Distinct effects of losartan and atenolol on vascular stiffness in Marfan syndrome. *Vasc Med*. 2015;20:317–325.
51. Lacro RV, Dietz HC, Sleeper LA, Yetman AT, Bradley TJ, Colan SD, Pearson GD, Selamet Tierney ES, Levine JC, Atz AM, et al. Atenolol versus losartan in children and young adults with Marfan's syndrome. *N Engl J Med*. 2014;371:2061–2071.
52. Franken R, den Hartog AW, Radonic T, Micha D, Maugeri A, van Dijk FS, Meijers-Heijboer HE, Timmermans J, Scholte AJ, van den Berg MP, et al. Beneficial outcome of losartan therapy depends on type of FBN1 mutation in Marfan syndrome. *Circ Cardiovasc Genet*. 2015;8:383–388.
53. Pyeritz RE. Marfan syndrome: improved clinical history results in expanded natural history. *Genet Med*. 2019;21:1683–1690.
54. Gallo EM, Loch DC, Habashi JP, Calderon JF, Chen Y, Bedja D, van Erp C, Gerber EE, Parker SJ, Sauls K, et al. Angiotensin II-dependent TGFβ signaling contributes to Loeys-Dietz syndrome vascular pathogenesis. *J Clin Invest*. 2014;124:448–460.

Supplemental Material

Figure S1. MFS phenotype at 11 weeks - Extravascular MFS features; Weight gain.

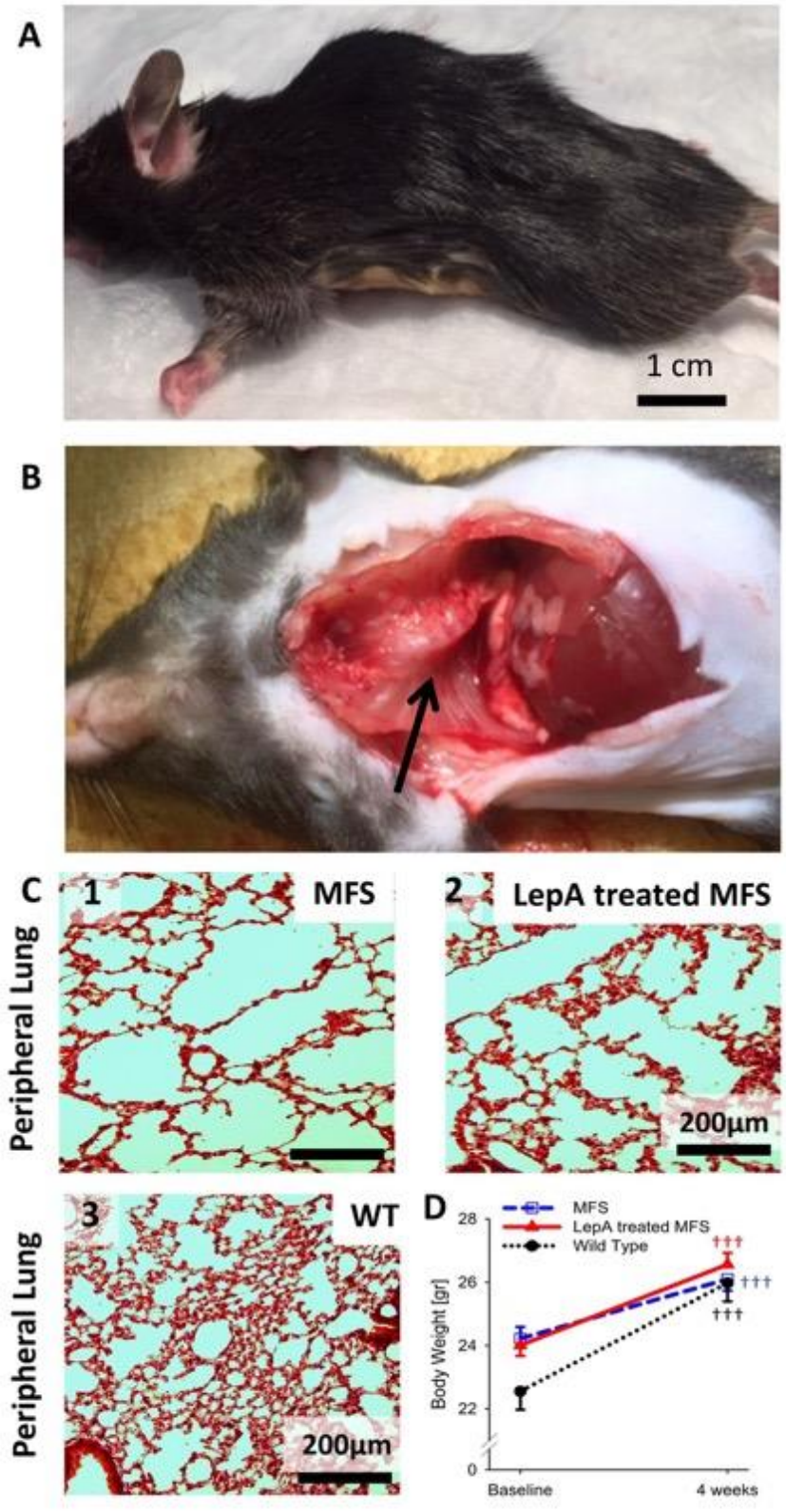

Kyphoscoliosis in Fbn1$^{C1039G/+}$ mouse (A), also deformed spine visualized through an open chest (B) (arrow). Dilatation of peripheral lung air spaces in MFS mouse (C1), a, similar dilatation of air spaces in a LepA-treated MFS mouse (C2), vs. normal lung histology of peripheral lung segment in a sibling WT mouse (C3). Body weight in MFS, LepA-treated MFS and WT mice at baseline and after 4 weeks (D).

++ $p < 0.01$, MFS at 4 weeks vs. baseline; +++ $p < 0.001$, LepA-treated MFS or WT at age 11 weeks vs. baseline.

*** $p < 0.001$, LepA-treated MFS vs. MFS at 4 weeks; +++ $p < 0.001$, MFS or LepA-treated MFS at 4 weeks vs. baseline; ### $p < 0.001$, MFS or LepA-treated MFS vs. WT.

Figure S2. IHC results of pSmad2, ACE-2 and AT1R expression in LV from MFS, LepA-treated MFS and WT mice.

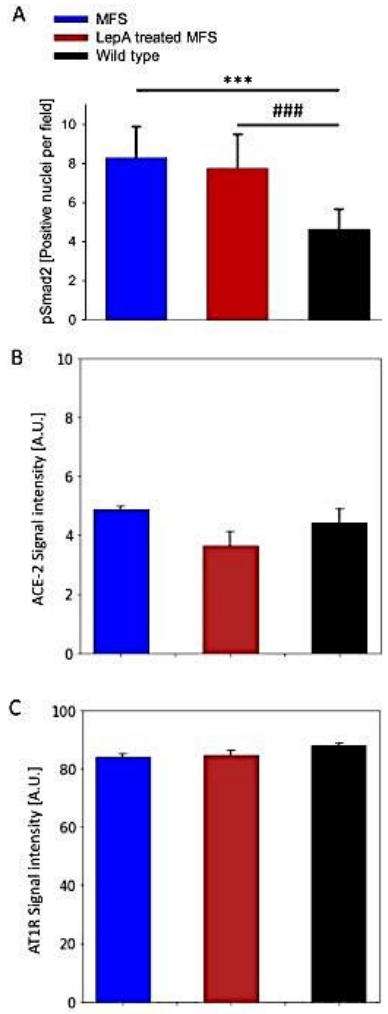

A. pSmad2 expression (number of positive nuclei per field). Note, MFS vs. LepA-treated MFS yielded insignificant statistical difference

B. ACE-2 expression. Insignificant statistical difference

C. AT1R expression. Insignificant statistical difference.